Anisotropic interface depinning: Numerical results

Heiko Leschhorn*
Center for Polymer Studies and Department of Physics, Boston University, Boston, Massachusetts 02215
(Received 21 December 1995; revised manuscript received 29 April 1996)

We study numerically a stochastic differential equation describing an interface driven along the hard direction of an anisotropic random medium. The interface is subject to a homogeneous driving force, random pinning forces, and surface tension. In addition, a nonlinear term due to the anisotropy of the medium is included. The critical exponents characterizing the depinning transition are determined numerically for a one-dimensional interface. The results are the same, within errors, as those of the ''directed percolation depinning'' (DPD) model. We therefore expect that the critical exponents of the stochastic differential equation are exactly given by the exponents obtained by a mapping of the DPD model to directed percolation. We find that a moving interface near the depinning transition is not self-affine and shows a behavior similar to the DPD model. [S1063-651X(96)11508-7]

PACS number(s): 05.40.+j, 75.60.Ch, 47.55.Mh, 74.60.Ge

I. INTRODUCTION

The driven viscous motion of an elastic interface in a medium with random pinning forces is relevant for the understanding of various problems in condensed matter physics [1]. Examples include the ordering dynamics of an impure Ising magnet after a quench below the critical temperature [2], wetting immiscible displacement of one fluid by another in a porous medium [3], and pinning of flux lines in type-II superconductors [4,5]. In recent years, studies of fluid imbibition in paper [6,7] and of flameless paper burning [8] have been carried out, and observable interfaces allow a direct comparison with theoretical predictions.

Common to all of these problems is a competition between smoothening due to the surface tension and roughening due to the interaction with the random pinning forces of the medium. Further, there is a competition between the driving force and the pinning forces, resulting in a depinning transition.

On a coarse-grained level, it is expected that the dynamics of the interface can be described by the following continuum equation of motion:

$$v_n(\vec{r},t)=\gamma K(\vec{r})+F+\eta(\vec{r})+\vec{n}\cdot\vec{\nabla}V(\vec{r}). \tag{1}$$

Here, $v_n(\vec{r},t)$ is the normal velocity of the interface at position $\vec{r}$. The surface tension generates a term proportional to the total curvature $K(\vec{r})=-\vec{\nabla}\cdot\vec{n}$, where $\vec{n}$ is the normal vector on the interface at $\vec{r}$. The coefficient γ measures the stiffness of the interface. F is a homogeneous driving force. The last two terms, $\eta(\vec{r})$ and $\vec{n}\cdot\vec{\nabla}V(\vec{r})$, represent random-field and random-bond disorder, respectively. The random forces $\eta(\vec{r})$ and the random potential $V(\vec{r})$ are short-range correlated in space.

Equation (1) is considerably simplified by restricting ourselves to an almost planar interface without overhangs. A coordinate system $\vec{r}=(\mathbf{x},h)$ can be introduced, so that the interface position is given by a single-valued function $h(\mathbf{x},t)$. The dimension of $\mathbf{x}$ is denoted by d. Equation (1) becomes [9]

$$\frac{1}{\sqrt{g}}\frac{\partial h(\mathbf{x},t)}{\partial t}=\gamma\nabla\cdot(g^{-1/2}\nabla h)+F+\eta(\mathbf{x},h)+\frac{1}{\sqrt{g}}\left[\nabla h\nabla V(\mathbf{x},h)-\frac{\partial V(\mathbf{x},h)}{\partial h}\right], \tag{2}$$

where $g=1+(\nabla h)^2$.

For sufficiently large values of the driving force F, the interface grows continuously. However, for smaller values of F, growth on some regions of the interface can come to a halt, due to the interaction with the quenched disorder. We say that these regions of the interface have become *pinned*. As the rest of the interface continues to grow, the pinned regions can be dragged over the pinning barriers by neighboring moving regions. Then, the formerly pinned regions advance quickly, which can be considered an avalanche [10–13].

The maximum linear size ξ of the pinned regions diverges when F approaches its critical value F_c,

$$\xi\sim|F-F_c|^{-\nu}. \tag{3}$$

The threshold F_c is the critical point of a dynamical phase transition, and ξ the corresponding correlation length. The role of the order parameter is played by the mean velocity, $v=\lim_{t\to\infty,L\to\infty}\overline{\partial h/\partial t}$. ($L$ is the system size and the overbar denotes the spatial average over $\mathbf{x}$.) The velocity is zero for $F<F_c$, and increases as

$$v\sim(F-F_c)^{\theta} \tag{4}$$

for F close to F_c. On length scales $l\gg\xi$ pinning can be neglected and we can therefore replace the argument h in the disorder terms $\eta(\mathbf{x},h)$ and $V(\mathbf{x},h)$ by vt; i.e., the quenched disorder crosses over to thermal noise [14]. Then, the interface is governed by the Kardar-Parisi-Zhang (KPZ) equation

*Present address: Theoretische Physik III, Heinrich-Heine-Universität Düsseldorf, D-40225 Düsseldorf, Germany.

[15]. In this paper, we are interested in the critical behavior on length scales $l \ll \xi$, especially when $\xi \to \infty$ at the depinning transition.

The global interface width $w^2 = \langle \overline{h(\mathbf{x},t) - h(t)}^{\,2} \rangle$ is another characteristic quantity of the interface. Here and elsewhere, $\langle\rangle$ denotes an average over the disorder distribution. Choosing a flat interface as the initial condition, $h(\mathbf{x},t=0) \equiv 0$, w^2 scales as [16,17]

$$w^2(\xi,t) \sim \xi^{2\alpha} \Psi_{\pm}(t/\xi^z) \tag{5}$$

for a sufficiently large system size, $L > \xi$. If $L < \xi$, the correlation length ξ in Eq. (5) has to be replaced by L. $\Psi_+(y)$ and $\Psi_-(y)$ are scaling functions for $F > F_c$ and $F < F_c$, respectively. Both functions scale as $\Psi_{\pm}(y) \sim y^{2\beta}$ for $y \ll 1$, where $\beta = \alpha/z$. It follows that

$$w^2(t) \sim t^{2\beta} \quad (t \ll \xi^z). \tag{6}$$

For $F > F_c$, pinning is irrelevant on length scales $l \gg \xi$, so we can neglect pinning also on time scales $t \gg \xi^z$. Thus, $\Psi_+(y) \sim y^{2\beta_m}$ for $y \gg 1$, where β_m is the growth exponent of an interface subject to thermal noise. Below threshold, the interface becomes pinned and $\Psi_-(y) = \text{const}$. Using the scaling of $\Psi_{\pm}(y)$ for $y \ll 1$ and Eq. (5) we obtain

$$w^2(\xi,t) \sim \begin{cases} t^{2\beta_m} & (t \gg \xi^z, \quad F > F_c) \\ \xi^{2\alpha} & (t \gg \xi^z, \quad F < F_c). \end{cases} \tag{7}$$

It has been shown that the critical exponents fulfill an exact scaling relation [14],

$$\theta = \nu(z - \alpha). \tag{8}$$

II. THE MODEL FOR ANISOTROPIC DEPINNING

To further simplify the equation of motion (2), we assume that the typical gradients ∇h are small on large length scales, so that the roughness exponent α is smaller than one. This assumption has to be compared with the final results. When expanding $1/\sqrt{g} \simeq 1 - (\nabla h)^2/2$, nonlinear terms proportional to $(\nabla h)^2$ are generated in Eq. (2). A natural question is whether these terms are relevant at the depinning transition. A term $(\nabla h)^2$ with a positive coefficient on the right-hand side of Eq. (2) would give a nonzero contribution to the driving force for any rough interface. This contribution increases when imposing a global tilt of the interface. Thus, the threshold F_c becomes a function of the average orientation of the interface. This is reasonable for anisotropic systems but not for isotropic ones. For interfaces in an isotropic environment, it can indeed be shown that the nonlinear terms generated by expanding $1/\sqrt{g}$ in Eq. (2) are irrelevant close to the depinning transition [11]. If, however, the medium is anisotropic, a term of the form $\lambda(\nabla h)^2$ can be relevant even for the case $v \to 0$. In fact, Tang, Kardar, and Dhar [9] argued that if ∇V and $\partial V/\partial h$ are differently distributed, the term $\lambda(\nabla h)^2$ is generated under coarse graining. More generally, if the system is anisotropic in the sense that the threshold F_c depends on the average orientation of the interface, $\lambda(\nabla h)^2$ is the only relevant term that can change the universality class of the depinning transition [9]. Motivated by these observations, we consider the following equation of motion:

$$\frac{\partial h(\mathbf{x},t)}{\partial t} = \gamma \nabla^2 h + \lambda(\nabla h)^2 + F + \eta(\mathbf{x},h). \tag{9}$$

For $\lambda > 0$ the threshold F_c has a maximum for an interface without tilt, i.e., an interface with periodic boundary conditions in Eq. (9) is driven along the hard direction of the anisotropic medium [9].

Equation (9) is the model we study in this paper. For simplicity, we restrict ourselves to interface dimension $d = 1$ and consider only random-field disorder $\eta(x,h)$. It was shown by Narayan and Fisher [11] for isotropic systems that random fields and random bonds give rise to the same critical behavior. This has been supported by numerical simulations of interfaces subject to random-bond disorder [18,19]. The random forces are assumed to have zero mean and short-range correlations, $\langle \eta(x',h')\,\eta(x'+x,h'+h) \rangle = \delta(x)\Delta(h)$, where $\Delta(h)$ decreases exponentially for $|h|$ greater than a microscopic cutoff.

A. Previous results

The case $\lambda = 0$ in Eq. (9) was first investigated by Feigel'man [20]. Significant progress has been made by a functional renormalization-group treatment [11,14,21] and by extensive numerical simulations [13,21–25].

The results for the anisotropic case $\lambda > 0$ are less well established. It was first suggested in Ref. [26] that Eq. (9) is in the same universality class as the ''directed percolation depinning'' (DPD) model [6,17]. For $d = 1$, directed percolating paths of pinning sites stop the interface. Thus, the roughness of the pinned interface is given by the scaling of the directed paths and the corresponding roughness exponent is $\alpha \simeq 0.633$ [6,17]. The other critical exponents of the DPD model can also be obtained by a mapping to directed percolation; in $d = 1$ the dynamical exponent $z = 1$, the correlation length exponent $\nu \simeq 1.733$, and the velocity exponent $\theta \simeq 0.636$.

Amaral, Barabási, and Stanley [27] measured the tilt dependence of the velocity for several versions of the DPD model and found a behavior consistent with the relevance of the term $\lambda(\nabla h)^2$ at the depinning transition. Galluccio and Zhang [28] simulated a self-organized version [29,30] of Eq. (9) and obtained $\alpha \simeq 0.63$, thereby supporting the conjecture of Ref. [26]. Recently, Olami, Procaccia, and Zeitak [25] argued that the slopes of the pinned surfaces in Eq. (9) are bounded and that therefore Eq. (9) could belong to the directed percolation universality class.

However, Csahók *et al.* [31] performed the only direct simulation of the continuum equation (9) and came to a different conclusion: Their numerical values for the exponents α and β in $d = 1$ are in agreement with a scaling theory for Eq. (9), which yields $\alpha = (4-d)/4$ and $\beta = (4-d)/(4+d)$ [31]. Yet another proposal was made by Parisi [32]. He argued that $\beta = (4-d)/4$ and supported this value in $d = 1$ by a simulation of a lattice model, which was assumed to be in the universality class of Eq. (9). Problematic is also the interpretation of Stepanow's renormalization-group calculation

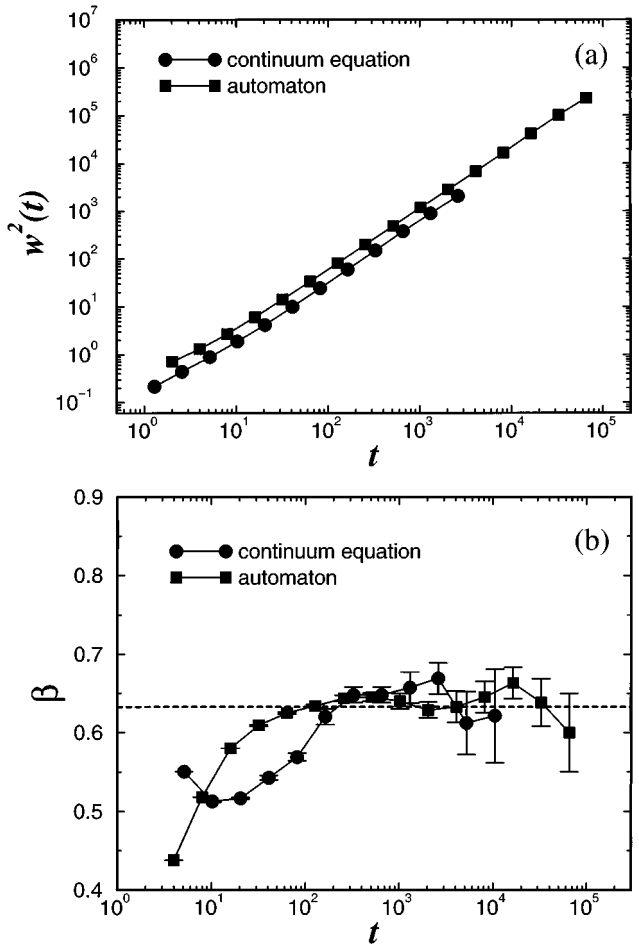

FIG. 1. (a) Scaling of the interface width $w^2(t) \sim t^{2\beta}$ at threshold. Interfaces of size $L = 16\,384$ at $F_c \simeq 0.1511$ were simulated for the continuum equation (10), and at $p_c \simeq 0.6631$ for the automaton ($L = 262\,144$). The data were averaged over 40 independent disorder distributions. The statistical uncertainties are smaller than the size of the symbols. The asymptotic slopes yield $\beta = 0.64 \pm 0.02$ for both lines. (b) The corresponding effective exponents $\beta(t) = \ln[w^2(t)/w^2(t/2)]/\ln 4$. The value $\beta \simeq 0.633$ of the DPD model is shown as the dashed horizontal line.

in $d = 4 - \epsilon$ dimensions [33]. The extrapolation to $d = 1$ gives the results $\alpha \simeq 0.86$, $z \simeq 1$, $\nu \simeq 1.2$, and $\theta \simeq 0.16$ [33].

B. Aim of the paper

To resolve these discrepancies we carefully determine in this paper the critical exponents by large-scale simulations of Eq. (9) for interface dimension $d = 1$. To this end we carry out a numerical integration of the equation of motion with a continuous height variable as well as a simulation of an automaton model where the height variable takes integer values only. In addition to the previously measured exponents α and β we also determine the exponents ν and θ to strengthen our conclusions. We find that the numerical values for all critical exponents are in agreement with the suggestion that Eq. (9) and the DPD model belong to the same universality class.

In addition, we investigate the interface roughness for $F > F_c$. It is shown that a moving interface is not self-affine

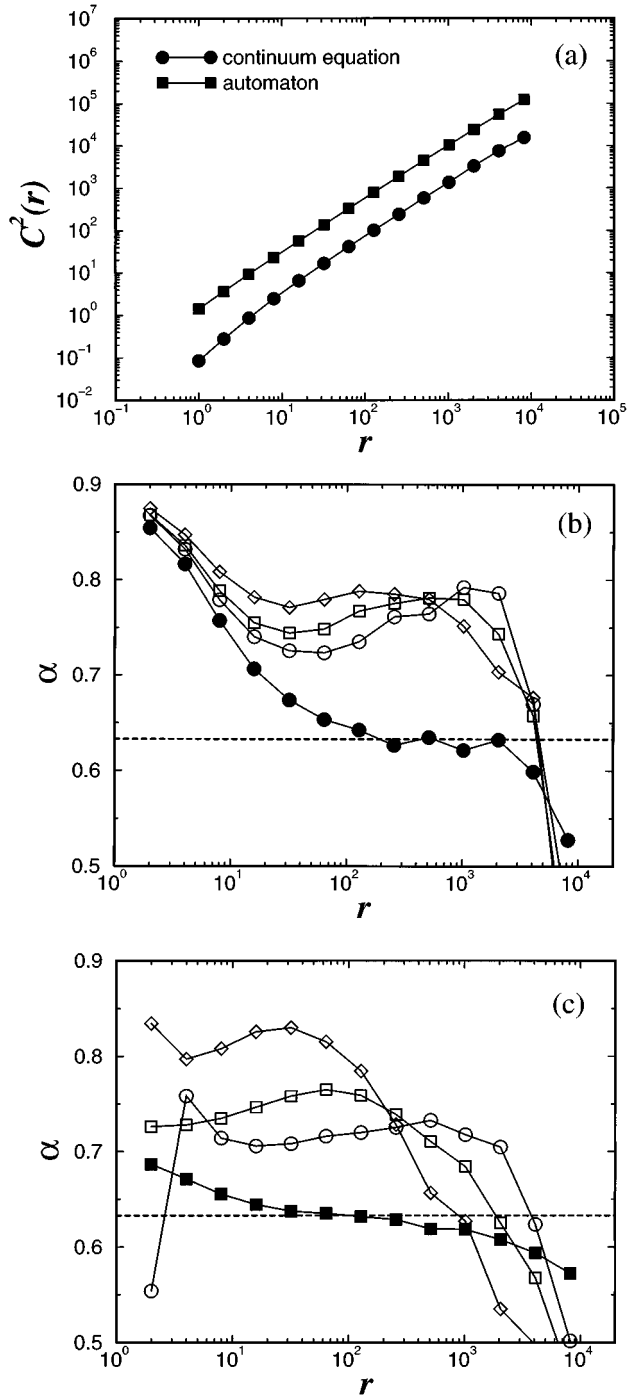

FIG. 2. (a) Equal-time correlation function $C^2(r) \sim r^{2\alpha}$ for pinned interfaces slightly below threshold: $F = 0.149$ ($L = 65\,536$) for Eq. (10) and $p = 0.6623$ ($L = 131\,072$) for the automaton. We averaged the data over 12 independent runs. Both lines give $\alpha = 0.63 \pm 0.01$. (b) Critical effective exponents $\alpha(r) = \ln[C^2(r)/C^2(r/2)]/\ln 4$ corresponding to (a) for the continuum equation (full symbols). The dashed line indicates the exponent $\alpha \simeq 0.633$ of the DPD model. In addition, the effective exponents $\alpha_q(r)$ for different moments q of the equal-time correlation function $C^q(r)$ for moving interfaces above threshold ($F = 0.157$, $L = 32\,768$) are shown: $q = 1$ (open circles), $q = 2$ (open squares), and $q = 4$ (open diamonds). The data were averaged over 30 disorder distributions so that the statistical uncertainties are of the size of the symbols or smaller. (c) The same as (b) but for the automaton. The open symbols are the effective exponents for moving interfaces at $p = 0.665$ (30 disorder distributions with $L = 32\,768$).

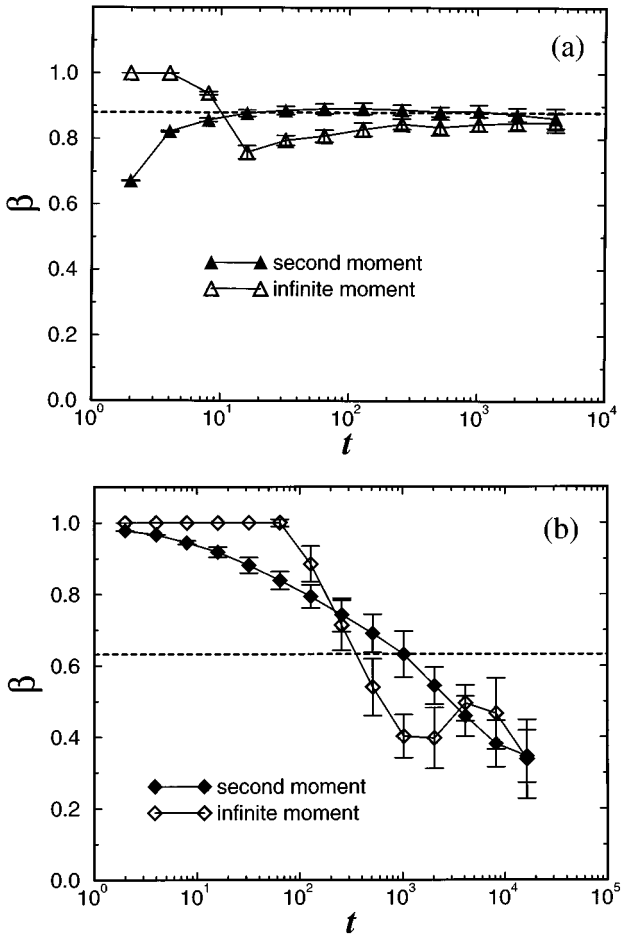

FIG. 3. (a) Effective exponents $\beta(\tau)$ (full symbols) for the automaton with $\lambda=0$, $\gamma=1$, $g=1$, $p=0.801>p_c\simeq 0.8004$, and $L=32\,768$. The data were averaged over 30 disorder distributions. The dashed line indicates the critical exponent $\beta\simeq 0.88$ [22] from a measurement of the global width at threshold. The effective exponents $\beta_\infty(\tau)$ (open symbols) seem to approach this value for large τ. (b) The same as (a) but for the DPD model of Ref. [17] with $p=0.467>p_c\simeq 0.461$ (30 runs with $L=32\,768$).

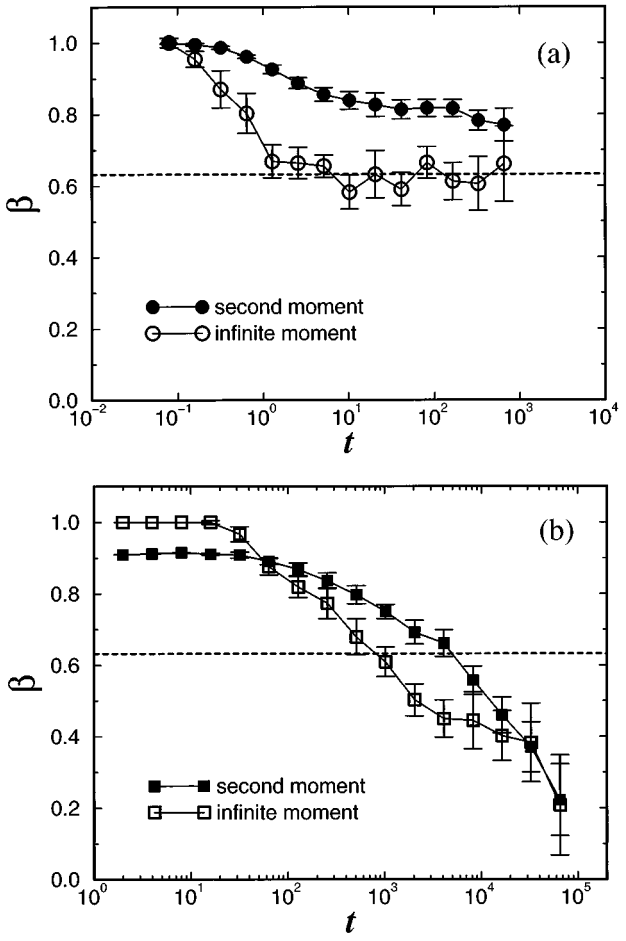

FIG. 4. (a) Effective exponents $\beta(\tau)$ and $\beta_\infty(\tau)$ for the continuum equation ($F=0.157>F_c\simeq 0.1511$, 30 runs with $L=32\,768$). (b) The same as (a) but for the automaton ($p=0.665>p_c\simeq 0.6631$, 30 runs with $L=32\,768$).

and that the behavior of the roughness is very similar to that of the DPD model.

III. NUMERICAL METHODS

A. Continuum equation

First we simulate Eq. (9) with a discretization of the transverse coordinate only, $x\to i$, $h(x,t)\to h_i(t)$ (with $1\leqslant i\leqslant L$). The random forces $\eta_i(h)$ are chosen as follows: Each integer position h_i on a square lattice is assigned a random number η between zero and one. For noninteger h_i the forces $\eta_i(h)$ are obtained by linear interpolation [32]. Finally, the h coordinates of $\eta_i(h)$ in each column i are shifted by a random amount $0\leqslant s_i<1$, i.e., $\eta_i(h)\to\eta_i(h+s_i)$ [34].

At $t=0$ the interface is flat, $h_i(t=0)\equiv 0$. The interface configuration at $t+\Delta t$ is calculated simultaneously for all i using the method of finite differences [35],

$$h_i(t+\Delta t)=h_i(t)+\Delta t\{\gamma[h_{i+1}(t)+h_{i-1}(t)-2h_i(t)]+\lambda[h_{i+1}(t)-h_{i-1}(t)]^2+g\,\eta_i(h_i)\}. \quad (10)$$

Periodic boundary conditions are used and g is a parameter measuring the strength of the disorder. We choose the parameters $\gamma=5$, $\lambda=1$, $g=3$ [36], and use $\Delta t=0.04$, for which Eq. (10) is found to be stable. We checked that simulations with $\Delta t=0.01$ yield consistent results.

B. Automaton model

Since the simulations of the continuum equation (10) are computationally expensive, we also study a lattice model [22] of probabilistic cellular automata, which allows one to determine the critical exponents more effectively.

The automaton model is defined on a square lattice where each cell $[i,h]$ (with $1\leqslant i\leqslant L$) is assigned a random force $\eta_{i,h}$, which takes the value 1 with probability p and $\eta_{i,h}=-1$ with probability $1-p$. During the motion at a given time t the local force

$$f_i(t)=\gamma[h_{i+1}(t)+h_{i-1}(t)-2h_i(t)]+\lambda[h_{i+1}(t)-h_{i-1}(t)]^2+g\,\eta_{i,h_i} \quad (11)$$

is determined for all i. The interface configuration is then updated simultaneously for all i [22]:

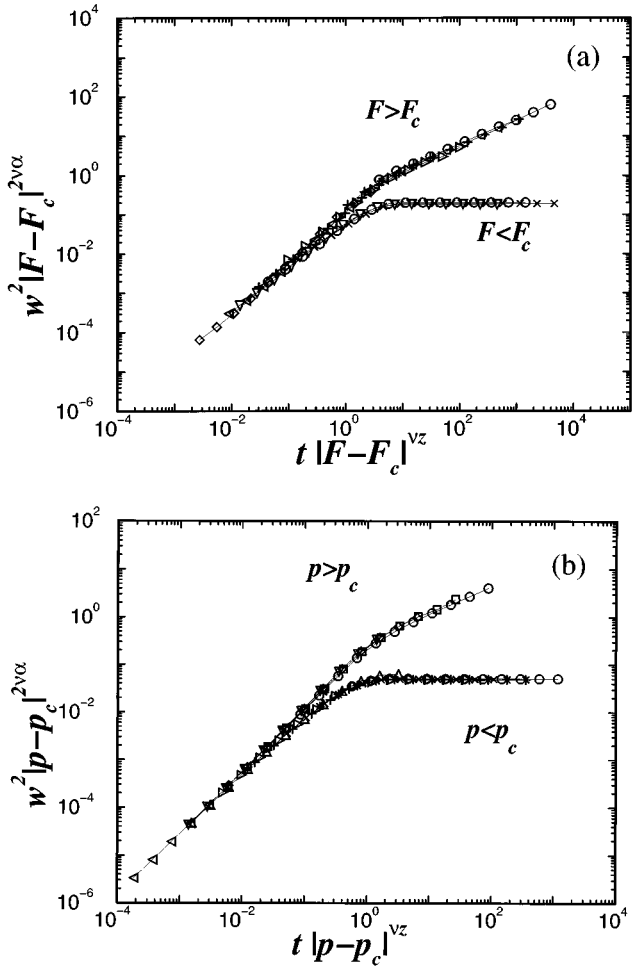

FIG. 5. (a) Scaling plot according to Eq. (5) for the continuum equation. The same plotting symbol is used for data at a given driving force F. Above threshold, F is in the range $0.163 \leqslant F \leqslant 1$ and below threshold $0.03 \leqslant F \leqslant 0.12$. For each value of F we simulated 50 independent runs with $L = 16\,384$. The best data collapse is achieved with $\alpha \simeq 0.63$, $z \simeq 1$, and $\nu \simeq 1.7$. (b) Scaling plot according to Eq. (5) for the automaton. Above threshold, p is in the range $0.664 \leqslant p \leqslant 0.695$ (20 independent runs) and below threshold $0.567 \leqslant p \leqslant 0.66$ (100 independent runs). The exponents for the best data collapse are $\alpha \simeq 0.63$, $z \simeq 1$, and $\nu \simeq 1.72$.

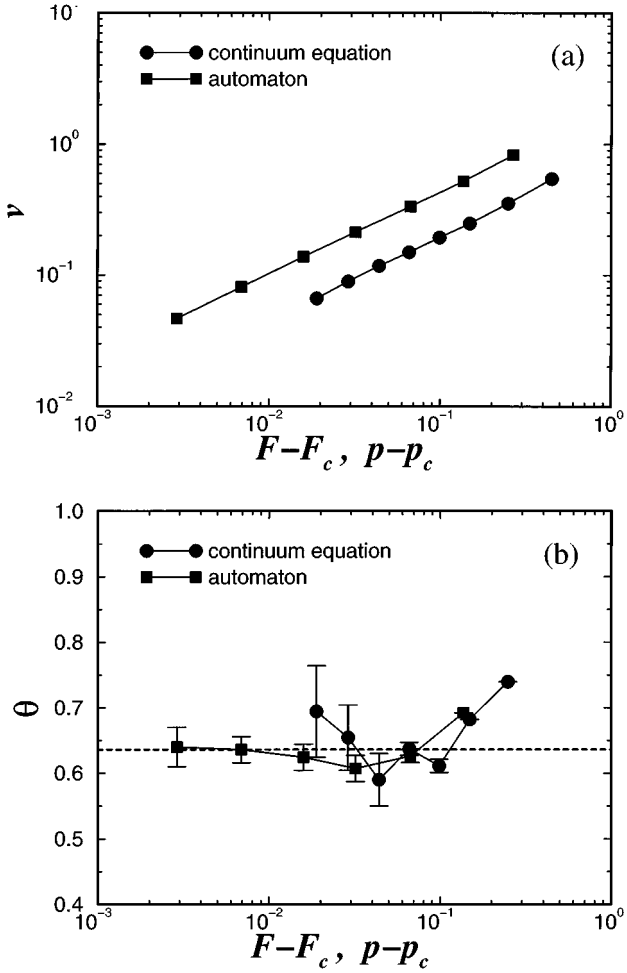

FIG. 6. (a) The interface velocity v as a function of the driving force. The velocity is averaged over sufficiently long time intervals, so that the statistical uncertainties are smaller than the size of the symbols. For the continuum equation we obtain $\theta = 0.64 \pm 0.05$ ($L = 65\,536$) and for the automaton $\theta = 0.63 \pm 0.02$ ($L = 131\,072$). (b) The effective exponents $\theta(F - F_c) = \ln[v(F)/v(F')]/\ln[(F - F_c)/(F' - F_c)]$. The dashed line indicates the critical value $\theta \simeq 0.636$ of the DPD model.

$$h_i(t+1) = \begin{cases} h_i(t) + 1 & \text{if } f_i > 0, \\ h_i(t) & \text{otherwise.} \end{cases} \tag{12}$$

The difference $p - (1-p) = 2p - 1$ determines the driving force. For simplicity, we use the density p as the tunable parameter, and the depinning threshold is denoted by p_c. The results shown in this paper were performed with the parameters $\gamma = 10$, $\lambda = 1$, and $g = 20$ [36].

The growth rule specified by Eqs. (11) and (12) can be derived from the continuum equation (9) by temporal and spatial discretizations. In addition, a simple two-state random force $\eta_{i,h} = \pm 1$ is used. The discretization implies that the critical slowing down close to the threshold is reduced. This can be seen as follows. For $v \to 0$, the local force for most of the interface elements $h_i(t)$ in Eq. (10) is almost zero. Nonetheless, in the finite difference approximation Eq. (10), all $h_i(t)$ and $\eta_i(h_i)$ have to be updated at each time step. On the other hand, only a subset of values $h_i(t)$ and η_{i,h_i} are updated at each time step in the cellular automata model.

IV. NUMERICAL RESULTS

A. Roughness at threshold

In this section we determine the critical exponents α and β, defined in Eqs. (5) and (6), respectively. First we find the threshold value F_c and p_c from a measurement of the interface width $w^2(t)$ for different values of the driving force. Since the correlation length increases when $F \to F_c$, the range of the scaling regime $w^2(t) \sim t^{2\beta}$ also increases [see Eq. (6)]. The threshold is estimated as the value where the power-law scaling holds for the longest time interval. This method allows one to determine the threshold very accurately.

In Fig. 1(a) the width $w^2(t)$ at the estimated threshold is shown in the transient regime, $t \ll \xi$. In Fig. 1(b) the corresponding effective exponents $\beta(t) = \ln[w^2(t)/w^2(t/2)]/\ln 4$ are

shown. Plotting the effective exponents $\beta(t)$ sensitively shows the quality of the power-law scaling. From Fig. 1 we conclude that $\beta=0.64\pm0.02$ for both the continuum equation (10) and the automaton [Eqs. (11) and (12)]. This is in very good agreement with the value $\beta\simeq0.633$, obtained by mapping the DPD model to directed percolation [6,17].

A convenient estimate of the roughness exponent α can be obtained by measuring the equal-time correlation function $C^2(r,t)=\langle\overline{[h_{i+r}(t)-h_i(t)]^2}\rangle$ of pinned interfaces. In Fig. 2(a), the scaling $C^2(r)\sim r^{2\alpha}$ for $r\ll\xi$ and F slightly below F_c is shown. The corresponding effective exponents $\alpha(r)=\ln[C^2(r)/C^2(r/2)]/\ln4$ are plotted in Figs. 2(b) and 2(c). Equation (10) and the automaton yield the same result, $\alpha=0.63\pm0.01$, again in agreement with the prediction of directed percolation, $\alpha\simeq0.633$. Using the numerical result for β, we see that the simulations are also consistent with $z=\alpha/\beta=1$ [6,17].

B. Roughness above threshold

In this section we consider the steady-state behavior of the roughness for moving interfaces at driving forces $F>F_c$ such that $\xi<L$. We are interested in the large-time limit, $t\gg\xi^z$, when the instantaneous velocity of the interface fluctuates around its mean value v.

Recently, it was proposed that the roughness of moving interfaces in the DPD model exhibits scaling with exponents different from the critical ones [24]. This is in disagreement with Ref. [17], where it was argued that on scales $l\ll\xi$, the moving interfaces are *not* self-affine because they consist of pinned regions with $\alpha\simeq0.63$ and laterally moving regions with roughly linear slopes ($\alpha\simeq1$). As a consequence, different moments of the equal-time correlation function, $C^q(r,t)=\langle\overline{|h_{i+r}(t)-h_i(t)|^q}\rangle$, yield different effective roughness exponents, $\alpha_q(r)=\ln[C^q(r)/C^q(r/2)]/[q\ln2]$.

We measure $C^q(r,t)$ for the continuum equation (10) and for the automaton and find results very similar to the DPD model [17] [see Figs. 2(b) and 2(c)]. The effective exponents $\alpha_q(r)$ increase with q. The reason is that the moving regions (large slopes) have an increasing weight with increasing q [17].

Another possibility to investigate the scaling of moving interfaces is a measurement of the height-height correlation function, $c^2(\tau)=\langle\overline{[h_i(t+\tau)-h_i(t)]^2}\rangle$, for $t\gg\xi^z$ and $\xi<L$. For $\tau\ll\xi^z$, the height-height correlation function scales as $c^2(\tau)\sim\tau^{2\beta}$, provided the interface is self-affine. As an illustration we consider the case $\lambda=0$.

1. Height-height correlation function for the case $\lambda=0$

The growth exponent β has been determined in Refs. [22,24] by simulations of the automaton model, Eqs. (11) and (12), with $\lambda=0$. The scaling of the interface width at threshold, Eq. (6), yields $\beta\simeq0.88$ [22] and $\beta\simeq0.85$ [24]. Here, we measure the effective exponents in the steady-state regime, $\beta(\tau)=\ln[c^2(\tau)/c^2(\tau/2)]/\ln4$. They are approximately constant over three orders of magnitude of τ, with $\beta=0.88\pm0.01$ [see Fig. 3(a)]. The effective exponent $\beta_\infty(\tau)$ of the infinite moment of the height-height correlation function, $c_\infty(\tau)=\langle\max_i\{h_i(t+\tau)-h_i(t)\}\rangle\sim\tau^{\beta_\infty}$, is also shown in Fig. 3(a). The effective exponent $\beta_\infty(\tau)$ increases slightly for $\tau\gtrsim16$ and approaches a value β_∞, which is consistent with the values of Refs. [22] and [24] obtained by the width at threshold. We conclude that the interface in Eq. (9) with $\lambda=0$ is self-affine with the same growth exponent β for both $F=F_c$ and $F>F_c$.

2. Height-height correlation function for the anisotropic case

In contrast, the same measurement for the DPD model [see Fig. 3(b)] gives decreasing effective exponents $\beta(\tau)$ and $\beta_\infty(\tau)$, which shows that there is no scaling with the critical growth exponent $\beta\simeq0.63$. For small times τ, the effective exponents $\beta(\tau)$ and $\beta_\infty(\tau)$ are roughly 1, which can be understood from the lateral motion of the parts of the interface with linear slope. The behavior of the automaton with $\lambda>0$ is very similar [see Fig. 4(b)]. The effective exponent $\beta(\tau)$ for the continuum equation [Fig. 4(a)] also decreases with τ but shows a plateau at a value $\beta\simeq0.82$. The infinite moment $c_\infty(\tau)$ seems to show a scaling for large τ with $\beta_\infty\simeq0.63$. It is not clear whether or not these plateaus in Fig. 4(a) can be considered as some (multi) scaling regime. We can only conclude that the behavior is different from that of a self-affine interface, which is characterized by the same critical growth exponent β for $F=F_c$ and $F>F_c$ as long as time scales $\tau\ll\xi^z$ are considered.

C. Scaling of the correlation length and the velocity

We now proceed to determine the correlation length exponent ν and the velocity exponent θ, which characterize the behavior of the interface close to the depinning transition.

In Fig. 5, scaling plots according to Eqs. (3) and (5) are shown. Since we already determined the threshold and the critical exponents α and $z=\alpha/\beta$, we can tune the correlation length exponent ν to achieve the best data collapse. The result for Eq. (10) is $\nu=1.7\pm0.1$ and for the automaton $\nu=1.72\pm0.03$. The corrections to the scaling $w^2(\xi)\sim\xi^{2\alpha}$ due to finite size effects are much larger for the continuum equation. Therefore simulations very close to the threshold are not shown in Fig. 5(a) and the error bar on the result for ν is rather large. The results for the correlation length exponent are consistent with the prediction of directed percolation, $\nu\simeq1.733$.

The growth exponent β_m defined in Eq. (7) for driving forces $F>F_c$ and time scales $t\gg\xi^z$ is found to be $\beta_m=0.32\pm0.03$ for the continuum equation and $\beta_m=0.32\pm0.02$ for the automaton. These values for β_m are consistent with the exponent $\beta_m=1/3$ of the KPZ equation [15]. This supports the picture that the quenched disorder $\eta(x,h)$ crosses over to a thermal noise $\eta(x,vt)$ on time scales $t\gg\xi^z$ (see Fig. 5).

The scaling of the steady-state velocity v Eq. (4) and the corresponding effective exponents θ are shown in Fig. 6. The result for the continuum equation is $\theta=0.64\pm0.05$, and $\theta=0.63\pm0.02$ for the automaton, again in agreement with the value of the DPD model, $\theta\simeq0.636$ [17].

V. SUMMARY AND CONCLUSIONS

The results for the roughness of Eq. (9) with and without the term $\lambda(\nabla h)^2$ are summarized in Table I.

For $\lambda>0$, pinned interfaces at $F=F_c$ are self-affine with

TABLE I. Behavior of the roughness for Eq. (9) in $d=1$.

	Eq. (9) with $\lambda=0$	Eq. (9) with $\lambda>0$
$F=F_c$, $v\to 0$	$\beta\simeq 0.88$ [22]	$\alpha\simeq\beta\simeq 0.63$
$F>F_c$, $v=\text{const}>0$, $\tau\ll\xi^z$	$\beta\simeq 0.88$	Not self-affine
$F>F_c$, $t\gg\xi^z$	$\beta_m=1/4$ [22]	$\beta_m=1/3$

a roughness exponent $\alpha\simeq 0.63$. Moving interfaces are not self-affine, which we demonstrated by measuring the correlation functions $C^q(r,t)$ and $c(\tau)$ (see Figs. 2–4). This is in comparison to the simpler behavior of Eq. (9) with $\lambda=0$, where not only pinned interfaces are self-affine (on length scales $l\ll\xi$) but also moving interfaces on time scales $\tau\ll\xi^z$. The latter can be seen from the fact that the height-height correlation function $c(\tau)$ for an interface moving with constant velocity scales with the same growth exponent $\beta\simeq 0.88$ as the global width at $F=F_c$ [see Fig. 3(a) and Table I]. The values for the exponent β_m [Eq. (7)] are obtained by the scaling of the global width $w(t)$ on time scales $t\gg\xi^z$ and correspond to those of the Edwards-Wilkinson equation ($\lambda=0$) [37] and the KPZ equation ($\lambda>0$) [15], respectively.

The results for the critical exponents characterizing the depinning transition of Eq. (9) with $\lambda>0$ are summarized in Table II.

The numerical results for both the continuum equation (10) and the automaton are in excellent agreement with the DPD model. We therefore expect that the critical exponents of the anisotropic depinning model Eq. (9) are exactly given by the exponents of directed percolation.

In the DPD model, the dynamic and the static behavior is determined by directed percolation paths of pinning sites. Due to the restricted solid-on-solid condition of the directed percolation paths, the pinned regions of the interface have small gradients (bounded by a slope one) [17]. In contrast, the laterally moving regions have a linear slope of about two [17]. This behavior is analogous to that of Eq. (9); regions of the interface with large slopes are likely to move due to the positive contribution of the term $\lambda(\nabla h)^2$ to the driving force. Regions of the interface with small gradients, on the other hand, are easier to pin, due to the smaller contribution of $\lambda(\nabla h)^2$.

TABLE II. Comparison of the critical exponents of the DPD model with our numerical results.

Exponent	DPD	Continuum eq.	Automaton
Roughness α	0.633	0.63 ± 0.01	0.63 ± 0.01
Growth β	0.633	0.64 ± 0.02	0.64 ± 0.02
Correlation length ν	1.733	1.7 ± 0.1	1.72 ± 0.03
Velocity θ	0.636	0.64 ± 0.05	0.63 ± 0.02

The observation that the interface motion is mainly due to the gradient term $\lambda(\nabla h)^2$ causes a clustering of growth sites, which can be understood as follows. A motion of an interface element $h(x)\to h(x)+dh$ increases the contribution of $\lambda(\nabla h)^2$ to the local force at $h(x+dx)$ or $h(x-dx)$. Thus, this neighboring interface element is likely to be the next new growth site, resulting in a cluster of growth sites to be formed. The moving regions have larger slopes than the pinned parts. As a consequence, a moving interface is not self-affine. The clustering of growth sites in Eq. (9) does not destroy the dynamical scaling of global quantities of the interface, such as the width and the velocity [see Eqs. (4)–(6)]. The scaling relation (8) is also fulfilled by the exponents of the DPD model and by our numerical results.

The behavior of moving interfaces deserves further investigation to understand better the concepts of scaling and self-affinity (see Sec. IV B). Further, it would be very interesting to construct a rigorous proof that Eq. (9) and the DPD model are in the same universality class.

ACKNOWLEDGMENTS

I would like to thank L. A. N. Amaral, P. Bak, S. V. Buldyrev, R. Cuerno, S. Galluccio, S. T. Harrington, S. Havlin, K. B. Lauritsen, H. A. Makse, M. Paczuski, H. E. Stanley, L.-H. Tang, and S. Zapperi for valuable discussions. I acknowledge support from the Deutsche Forschungsgemeinschaft. The Center for Polymer Studies is supported by the National Science Foundation.

[1] A.-L. Barabási and H. E. Stanley, *Fractal Concepts in Surface Growth* (Cambridge University Press, Cambridge, 1995).

[2] For reviews see, e.g., T. Nattermann and P. Rujan, Int. J. Mod. Phys. B **3**, 1597 (1989); D. P. Belanger and A. P. Young, J. Magn. Magn. Mater. **100**, 272 (1991); G. Forgacs, R. Lipowsky, and Th. M. Nieuwenhuizen, in *Phase Transitions and Critical Phenomena*, edited by C. Domb and J. L. Lebowitz (Academic, London, 1991), Vol. 14, p. 135.

[3] M. A. Rubio, C. A. Edwards, A. Dougherty, and J. P. Gollub, Phys. Rev. Lett. **63**, 1685 (1989); V. K. Horváth, F. Family, and T. Vicsek, J. Phys. A **24**, L25 (1991); S.-j. He, G. Kahanda, and P.-z. Wong, Phys. Rev. Lett. **69**, 3731 (1992).

[4] For reviews see, e.g., D. S. Fisher, M. P. A. Fisher, and D. A. Huse, Phys. Rev. B **43**, 130 (1991); G. Blatter, M. V. Feigel'man, V. B. Geshkenbein, A. I. Larkin, and V. M. Vinokur, Rev. Mod. Phys. **66**, 1125 (1994).

[5] D. Ertas and M. Kardar, Phys. Rev. Lett. **73**, 1703 (1994).

[6] S. V. Buldyrev, A.-L. Barabási, F. Caserta, S. Havlin, H. E. Stanley, and T. Vicsek, Phys. Rev. A **45**, R8313 (1992).

[7] V. K. Horváth and H. E. Stanley, Phys. Rev. E **52**, 5166 (1995).

[8] J. Zhang, Y.-C. Zhang, P. Alstrom, and M. T. Levinsen, Physica A **189**, 383 (1992).

[9] L.-H. Tang, M. Kardar, and D. Dhar, Phys. Rev. Lett. **74**, 920 (1995).

[10] A.-L. Barabási, S. V. Buldyrev, S. Havlin, G. Huber, H. E. Stanley, and T. Vicsek, in *Surface Disordering: Growth, Roughening, and Phase Transitions*, edited by R. Jullien, J. Kertész, P. Meakin, and D. E. Wolf (Nova Science, New York, 1992), p. 193.

[11] O. Narayan and D. S. Fisher, Phys. Rev. B **48**, 7030 (1993).
[12] Z. Olami, I. Procaccia, and R. Zeitak, Phys. Rev. E **49**, 1232 (1994); H. Leschhorn and L.-H. Tang, *ibid.* **49**, 1238 (1994).
[13] M. Paczuski, S. Maslov, and P. Bak, Phys. Rev. E **53**, 414 (1996).
[14] T. Nattermann, S. Stepanow, L.-H. Tang, and H. Leschhorn, J. Phys. (France) II **2**, 1483 (1992).
[15] M. Kardar, G. Parisi, and Y.-C. Zhang, Phys. Rev. Lett. **56**, 889 (1986).
[16] F. Family and T. Vicsek, J. Phys. A **18**, L75 (1985).
[17] L.-H. Tang and H. Leschhorn, Phys. Rev. A **45**, R8309 (1992).
[18] M. Dong, M. C. Marchetti, A. A. Middleton, and V. Vinokur, Phys. Rev. Lett. **70**, 662 (1993); H. Leschhorn and L.-H. Tang, *ibid.* **70**, 2973 (1993).
[19] H. J. Jensen, J. Phys. A **28**, 1861 (1995).
[20] M. V. Feigel'man, Zh. Eksp. Teor. Fiz. **85**, 1851 (1983) [Sov. Phys. JETP **58**, 1076 (1983)].
[21] H. Leschhorn, Ph.D. thesis, Ruhr-Universität Bochum, 1994; H. Leschhorn, T. Nattermann, S. Stepanow, and L.-H. Tang (unpublished).
[22] H. Leschhorn, Physica A **195**, 324 (1993).
[23] S. Roux and A. Hansen, J. Phys. (France) I **4**, 515 (1994).
[24] H. A. Makse and L. A. N. Amaral, Europhys. Lett. **31**, 379 (1995); L. A. N. Amaral, A.-L. Barabási, H. A. Makse, and H. E. Stanley, Phys. Rev. E **52**, 4087 (1995).
[25] Z. Olami, I. Procaccia, and R. Zeitak, Phys. Rev. E **52**, 3402 (1995).
[26] L.-H. Tang and H. Leschhorn, Phys. Rev. Lett. **70**, 3832 (1993).
[27] L. A. N. Amaral, A.-L. Barabási, and H. E. Stanley, Phys. Rev. Lett. **73**, 62 (1994).
[28] S. Galluccio and Y.-C. Zhang, Phys. Rev. E **51**, 1686 (1995).
[29] S. Havlin, A.-L. Barabási, S. V. Buldyrev, C. K. Peng, M. Schwartz, H. E. Stanley, and T. Vicsek, in *Growth Patterns in Physical Sciences and Biology*, edited by E. Louis, L. Sander, and P. Meakin (Plenum, New York, 1993).
[30] K. Sneppen, Phys. Rev. Lett. **69**, 3539 (1992).
[31] Z. Chahók, K. Honda, and T. Vicsek, J. Phys. A **26**, L171 (1993); Z. Chahók, K. Honda, E. Somfai, M. Vicsek, and T. Vicsek, Physica A **200**, 136 (1993).
[32] G. Parisi, Europhys. Lett. **17**, 673 (1992).
[33] S. Stepanow, J. Phys. (France) II **5**, 11 (1995).
[34] H. Leschhorn, J. Phys. A **25**, L555 (1992).
[35] Galluccio und Zhang [28] used a different discretization of the gradient term in Eq. (9), $\nabla h \rightarrow |h_i - h_{i+1}| + |h_i - h_{i-1}|$ [S. Galluccio (private communication)]. We believe that this is an unsuitable discretization causing a growth instability of Eq. (9): It has been observed in Ref. [28] that an interface element h_i will grow infinitely faster than the rest of the interface when the height difference of h_i to its neighbors exceeds a certain amount. It has been concluded in Ref. [28] that the anisotropic depinning model Eq. (9) is ill defined due to this instability. However, with the correct discretization in Eqs. (10) and (11) no growth instability occurs and Eq. (9) is well defined.
[36] The strength of the disorder g has to be significantly larger than λ to assure that the depinning transition occurs at a critical driving force greater than zero. The stiffness γ is chosen to have the same order of magnitude as g, so that the interface can become rough on length scales of the lattice constant. We checked that other parameters yield consistent results.
[37] S. F. Edwards and D. R. Wilkinson, Proc. R. Soc. London A **381**, 17 (1982).